TRANSITION METAL DOPING EFFECTS ON STRUCTURES AND RAMAN SCATTERING IN ZnO NANOPARTICLES

N.N. MUSAYEVA*[1], P.A. AHMADOVA[1,2], P.A. ASKEROVA[1]
[1]Azerbaijan Ministry of Science and Education, Institute of Physics, Baku, Azerbaijan
[2]Baku State University, Baku, Azerbaijan
Corresponding author: nmusayeva@physics.science.az

Copper- and nickel-doped zinc oxide ($Zn_{1-x}M_xO$, where M =Cu or Ni and x = 0.00–0.05) nanocrystals were successfully synthesized via a chemical co-precipitation method. The effects of Cu and Ni incorporation on the structural and vibrational properties of ZnO were systematically investigated using X-ray diffraction (XRD) and Raman spectroscopy. XRD analysis confirmed that all samples retained the hexagonal wurtzite structure, indicating successful substitutional doping, while weak secondary phase peaks corresponding to CuO and NiO were detected at higher dopant concentrations. Raman analysis revealed red shifts, band broadening, and increased intensity of higher-order modes, suggesting enhanced lattice strain, oxygen vacancy concentration, and phonon coupling upon doping. These findings show that low-level Cu and Ni doping effectively alters the local structure and phonon dynamics of ZnO.

Keywords: ZnO, Cu, Ni, XRD, Raman spectroscopy, co-precipitation
PACS: 32.30.Rj; 32.20.Fb

1. Introduction

Zinc oxide (ZnO) is a II–VI semiconductor with a hexagonal wurtzite crystal structure. It is widely studied for its exceptional optical, piezoelectric and gas-sensing properties [1-4]. The crystal lattice of ZnO consists of alternating planes of Zn^{2+} and O^{2-} ions stacked along the c-axis, resulting in strong spontaneous polarization and anisotropic bonding characteristics [5]. Due to its wide direct band gap (3.37 eV) and large exciton binding energy (~60 meV), ZnO is considered one of the most versatile functional oxides for use in optoelectronics, photocatalysis, transparent conductors and spintronic devices [6,7].

The structural, electronic and vibrational behaviour of ZnO can be effectively tailored by introducing foreign atoms or defects into its lattice. Of the various strategies, transition metal (TM) doping has proven to be particularly effective in adjusting the electrical conductivity, magnetic response and defect-related optical transitions of ZnO, all the while maintaining the stability of the wurtzite phase. [8]. Doping with Cu and Ni is of particular interest as their ionic radii (Cu^{2+} = 0.73 Å and Ni^{2+} = 0.69 Å) are close to that of Zn^{2+} (0.74 Å). This allows them to be incorporated into Zn sites with minimal structural disruption. However, this substitution process inevitably introduces local lattice strain, oxygen vacancies and other point defects, which have a significant impact on phonon dynamics and electron–phonon interactions.

This study aims to synthesize Cu- and Ni-doped ZnO nanocrystals via a controlled co-precipitation method, and to analyze their structural and vibrational characteristics in comparison to undoped ZnO. By correlating XRD and Raman results, the study will seek to elucidate the effects of transition metal incorporation on lattice strain, defect formation and phonon behaviour in ZnO nanoparticles.

2. Experimental

2.1. Synthesis of Cu- and Ni-doped ZnO NPs

$Zn_{1-x}M_xO$ (M =Cu (Ni); x = 0.00, 0.01, 0.05) nanocrystals were synthesized by one step co-precipitation method. Zinc chloride ($ZnCl_2$), copper (II) chloride dihydrate ($CuCl_2 \cdot 2H_2O$), and nickel (II) chloride hexahydrate ($NiCl_2 \cdot 6H_2O$) were used as metal precursors.

In a typical procedure, 0.05M of zinc chloride ($ZnCl_2$) was dissolved in deionized (DI) water under continuous magnetic stirring at a temperature of 60 °C and a stirring speed of 500 rpm. Subsequently, 20 mL of ethylene glycol was added as a stabilizing and capping agent, and the initial pH of the solution was adjusted to 4. An aqueous solution of sodium hydroxide (NaOH, 1.07 M) was then added dropwise over the course of 1 hour to initiate the precipitation process, during which the pH gradually increased to 6.1. The reaction temperature was subsequently raised to 90 °C, while the stirring speed was successively increased to 1000 rpm and then 1500 rpm toward the end of the reaction to ensure uniform nucleation and particle growth. The resulting precipitation was washed 3 times with DI water and centrifuged two times at 4000 rpm for 15 minutes each to remove residual ions and impurities. The obtained precipitate was then dried in a laboratory oven at 80 °C for 2 hours. Finally, the dried powder was calcined at 500 °C for 3 hours in a muffle furnace to obtain crystalline ZnO nanoparticles.

The synthesis of ZnO samples doped with 1% and 5% Cu (and Ni), was carried out under identical experimental conditions. The only difference was the addition of stoichiometrically calculated amounts of $CuCl_2 \cdot 2H_2O$ and $NiCl_2 \cdot 6H_2O$ to the $ZnCl_2$ solution during each separate reaction. Particular attention was paid to optimizing the pH value to ensure maximum precipitation during the synthesis process.

131, H.Javid ave, AZ-1073, Baku
Institute of Physics
E-mail: jophphysics@gmail.com

3. Results and Discussion

3.1. X-ray diffraction (XRD) analysis

XRD patterns of ZnO and 1% and 5% Cu doped ZnO samples are shown in Figure 1. All diffraction peaks correspond to the hexagonal wurtzite structure of ZnO (JCPDS card No. 36-1451), with characteristic reflections at 2θ ≈ 31.7°, 34.4°, 36.2°, 47.5°, 56.6°, 62.8°, 66.35, 67.9° and 69 assigned to the (100), (002), (101), (102), (110), (103), (200), (112) and (201) planes, respectively. As can be seen from Figure 1(a), the sample obtained by incorporating 1 at.% Cu into the ZnO matrix via the aforementioned chemical method shows almost no change in the diffraction pattern compared to pure ZnO. However, when 5 at.% of Cu is introduced, the primary crystalline phase remains hexagonal wurtzite-type ZnO, but very weak diffraction peaks are observed at around 2θ = 35.5° and 38.7°. This indicates the formation of a small amount of the monoclinic CuO phase. This behaviour indicates that Cu^{2+} ions primarily replace Zn^{2+} sites in the ZnO lattice, with only a small amount exceeding the solubility limit and forming a secondary CuO phase. Similar behaviour involving limited solubility of Cu in the ZnO lattice and subsequent formation of secondary CuO phases at higher concentrations has also been reported in the literature [9]. A similar trend is observed in the XRD patterns of ZnO doped with 1–5 at.% Ni (Figure 1b). Compared to pure ZnO, weak diffraction peaks appear at approximately 2θ ≈ 37.1° and 43.09° in the 1% Ni-doped ZnO sample and become more pronounced at 5% doping. This suggests that, while most Ni^{2+} ions substitute for Zn^{2+} ions in the ZnO lattice, a small fraction reacts with oxygen to form a partially compressed, strain-induced cubic NiO phase [10-12].

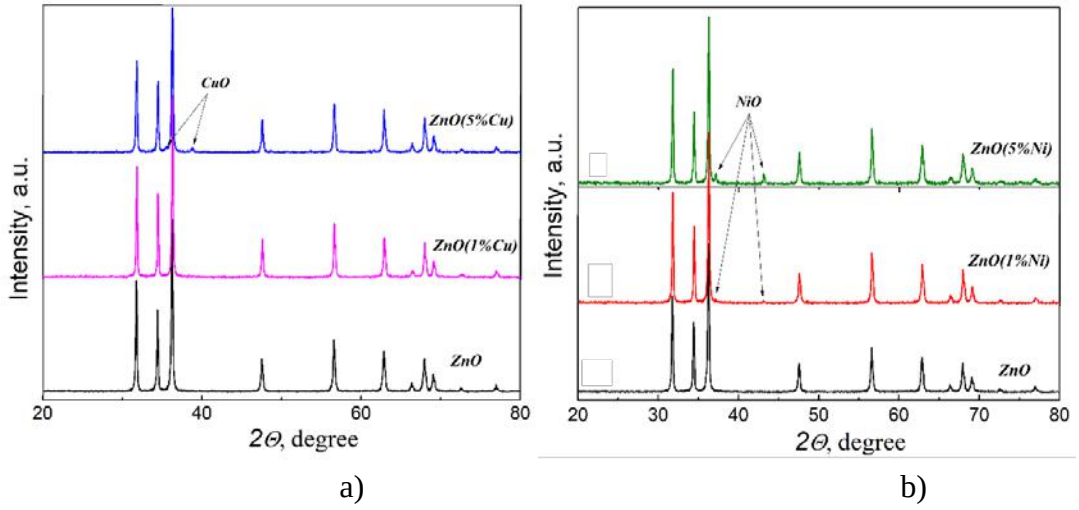

Fig. 1. X-ray diffraction of pure and metal doped ZnO NPs : a) Cu doped ZnO Ps; b) Ni doped ZnO NPs.

Further analysis revealed that the additional NiO peaks detected in Ni-doped samples were slightly shifted towards lower angles compared to the standard NiO positions. This shift is attributed to lattice expansion caused by internal strain and the generation of oxygen vacancies around the dopant ions. While Cu^{2+} (0.73 Å) is nearly the same size as Zn^{2+}, and thus induces minimal strain at lower doping levels, Ni^{2+} being smaller may generate more significant distortions in the lattice.

The average crystallite size, calculated from the intensive diffraction peaks using the Scherrer equation, was found to be ~33 nm for pure ZnO. Upon doping, the crystallite size increased slightly to ~35 nm for the 5% Cu-doped sample and decreased to ~30 nm for the 5% Ni-doped sample. This reduction in size for Ni doping suggests that the incorporation of Ni^{2+} ions hinders crystal growth by introducing lattice strain and structural defects. In contrast, the minimal lattice mismatch between Cu^{2+} and Zn^{2+} enables a small increase in crystallite size unless the Cu content exceeds the solubility limit, resulting in the formation of a secondary CuO phase.

3.2. Raman spectroscopy

Raman spectroscopy is a sensitive tool for investigating structural disorder, phonon confinement and dopant-induced effects in ZnO. Figure 2 shows the Raman spectra of pure ZnO and ZnO doped with Cu and Ni, recorded at room temperature in the range of 100–1400 cm^{-1}.

For the pure ZnO sample, the dominant Raman band observed at ~437 cm^{-1} corresponds to the E_2(high) mode, arising from the vibration of oxygen atoms in the wurtzite lattice. The weak feature near 333 cm^{-1} is attributed to a second-order Raman process: the E_2(high) − E_2(low) two-phonon difference mode. The band at ~380 cm^{-1} corresponds to the A_1(TO) mode, which is associated with the transverse optical vibration of Zn–O bonds. Additionally, the modes appearing near 578–585 cm^{-1} are characteristic of the A_1(LO) and E_1(LO) longitudinal optical phonons, which are typically enhanced by the presence of oxygen vacancies, donor-type defects or slight non-stoichiometry in ZnO [13,14]. A broad band centered around 1149 cm^{-1} also originates from a second-order two-phonon scattering process (2LO), which is characteristic of nanocrystalline ZnO.

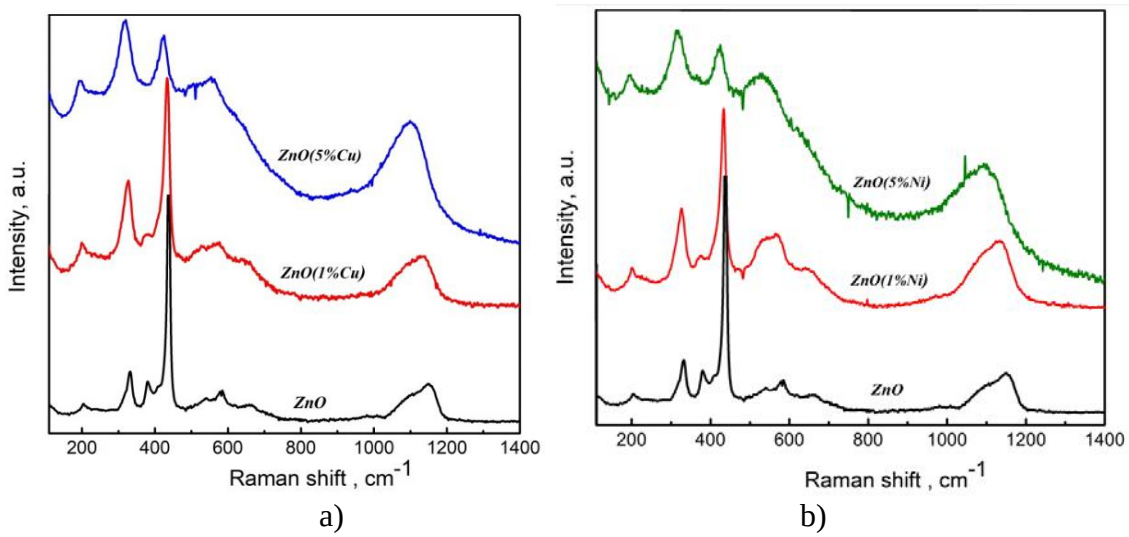

Fig. 2. Raman spectra of pure and metal doped ZnO NPs : a) Cu doped ZnO Ps; b) Ni doped ZnO NPs

Upon doping with Cu and Ni via the chemical method, significant spectral modifications were observed. In both cases, all Raman bands exhibited a red shift (a shift to lower wavenumbers), indicating lattice expansion and increased strain. The E_2(high) mode shifts from 437 cm^{-1} to ~424 cm^{-1} at a 5% dopant concentration, while the 333 cm^{-1} mode shifts to ~319 cm^{-1} (Cu) and ~316 cm^{-1} (Ni). Although the apparent intensity of the E_2(high) mode seems reduced, this effect is mainly due to overlap with neighbouring defect-related and LO modes rather than a true decrease in the phonon's intrinsic Raman activity. The observed red shift and the reduced separation between adjacent modes suggest increased lattice disorder and internal strain caused by dopant substitution within the ZnO matrix.

The E_1(LO) mode at around 584 cm^{-1} broadens and intensifies with increasing dopant concentration (x=0.01-0.05), reflecting growth in defect density and oxygen vacancy concentration. This is consistent with XRD results indicating lattice distortion. Furthermore, the high-wavenumber band at approximately 1149 cm^{-1}, which is assigned to the 2LO overtone, exhibits red-shifting and marked intensity enhancement upon Cu and Ni doping. This behaviour can be attributed to enhanced electron–phonon coupling and multiphonon scattering, facilitated by lattice strain and the formation of oxygen vacancies and point defects due to the incorporation of dopants.

4. Conclusion

In summary, structural and vibrational analyses confirmed the successful incorporation of both Cu and Ni into the ZnO lattice without disrupting its wurtzite crystal structure. Only minor traces of CuO and NiO phases were detected at higher dopant concentrations (5 at.%), indicating limited solubility of the dopants. The observed Raman shifts and line broadening reveal that metal incorporation induces local lattice distortion, increased defect density and stronger phonon–defect interactions. These effects suggest that strain induced by the dopants and oxygen vacancies play a key role in modifying the phonon dynamics of ZnO. Overall, the controlled incorporation of Cu and Ni is an effective approach for engineering the structural and optical properties of ZnO for use in advanced catalytic and functional applications.

[1] *S.B. Vijendra, M. Hojamberdiev, M. Kumar.* Enhanced sensing performance of ZnO nanostructures-based gas sensors: A review, Energy Reports, 6, S4, 2020, p 46-62, DOI: https://doi.org/10.1016/j.egyr.2019.08.070

[2] *W. Dai, X. Pan, C. Chen, S. Chen, W. Chen, H. Zhang, Z. Ye.* Enhanced UV detection performance using a Cu-doped ZnO nanorod array film, RSC Adv. 4, 2014, 31969, https://doi.org/10.1039/C4RA04249B.

[3] *P. Bandyopadhyay, A. Dey, R. Basu, S. Das, P. Nandy*. Synthesis and characterization of copper doped zinc oxide nanoparticles and its application in energy conversion, Curr. Appl. Phys. 14, 2014, 1149–1155, https://doi.org/10.1016/j.cap.2014.06.010

[4] *R. Sonkar, N.J. Mondal, B. Boro, M.P. Ghosh, D. Chowdhury*. Cu doped ZnO nanoparticles: correlations between tuneable optoelectronic, antioxidant and photocatalytic activities, J. Phys. Chem. Solids 185 (2024) 111715.

[5] *Ü. Özgür, Ya.I. Alivov, C. Liu.* et al., A comprehensive review of ZnO materials and devices. J. Appl. Phys., 98 (2005) 041301.

[6] *D.C. Look.* Recent advances in ZnO materials and devices. *Mater. Sci. Eng. B*, 80 (2001) 383–387.

[7] Klingshirn, ZnO: From basics towards applications C., Phys. Status Solidi B, 244 (2007) 3027–3073.

[8] *C. Jagadish, & S. Pearton.* Zinc Oxide Bulk, Thin Films and Nanostructures, Elsevier, 2006

[9] *S. David Jereil, S.M. Shankar, K Sudhakar*. Ganeshkumar Arumugam, Padmanaban Annamalai, Radhalayam Dhanalakshmi, Sreekanth T. V. M. , Abdullah Alarifi, Effect of Cu-ZnO nanoparticles on the photocatalytic degradation of reactive red 120, Surfaces and Interfaces, Volume 56, 2025, 105579, https://doi.org/10.1016/j.surfin.2024.105579 .

[10] *Nahida Musayeva, Arif Hashimov, Hadiya Khalilova, Bakhtiyar Izzatov, Sevinj Guluzade & Muhammad Alizada.* Enhancement effect of Ni and NiO on gas sensing characteristics of carbon nanotube based structures.// Fullerenes, Nanotubes and Carbon Nanostructures, 21 Aug 2023, DOI: 10.1080/1536383X.2023.2246165

[11] *M.B. Muradov, S.J. Mammadyarova, G.M. Eyvazova, O.O. Balayeva, N.N. Musayeva.* Sonochemical Synthesis and Characterization of Structural, Optical and Dielectric Properties of Ag-Doped Co3O4 Nanoparticles //Journal of Cluster Science 35 (3), 845-861 (2024) WoS/Q2, Scopus. İF-2.7 DOİ: https://doi.org/10.1007/s10876-023-02514-894

[12] *M.B Muradov, S.J Mammadyarova, G.M Eyvazova, O.O Balayeva, G Aliyeva, N.N.Musayeva.* Synthesis of Cu x Co 3− x O 4 nanoparticles by a sonochemical method and characterization of structural and optical properties and photocatalytic activity for the degradation. RSC advances 14 (2), 1082-1093 (2024), WoS/Q1, Scopus. İF- 3.9, DOİ:https://doi.org/10.1039/D2RA08060E

[13] *M. Šćepanovic, M. Grujić-Brojčin, K. Vojisavljević, S. Bernik, T. Srećković*. Raman study of structural disorder in ZnO nanopowders. J.Raman Spectrosc. Micro-Raman Investigation of Optical Phonons in ZnO Nanocrystals 41 (2010) 914. DOI: 10.1002/jrs.2546

[14] *K.A. Alim,V.A. Fonoberov, M. Shamsa, A.A. Balandin.* Micro-Raman Investigation of Optical Phonons in ZnO Nanocrystals. J.Appl.Phys.97(2005)124313.